

# Fabrication of Hydrophobic Graphene-Cellulose Composite Paper Using Rice Husk Ash Silica

Sariwahyuni<sup>1\*</sup>, Herlina Rahim<sup>2</sup>, Hanim Istatik Badi'ah<sup>3</sup>, Andi Haslinah<sup>4</sup>, & Mega Fia Lestari<sup>5</sup>

<sup>1\*</sup>Politeknik ATI Makassar, Indonesia, <sup>2</sup>Politeknik ATI Makassar, Indonesia, <sup>3</sup>UPN "Veteran" Jawa Timur, Indonesia, <sup>4</sup>Universitas Islam Makassar, Indonesia <sup>5</sup>Akademi Komunitas Industri Manufaktur Bantaeng, Indonesia

\*Co e-mail: sari.wahyuni@atim.ac.id1

# **Article Information**

Received: August 25, 2025 Revised: October 09, 2025 Online: October 16, 2025

## **Keywords**

Rice Husk Ash, Amorphous Silica, Graphene Nanoplatelets, Cellulose Composite Paper, Superhydrophobic

#### **ABSTRACT**

This study presents the fabrication and characterization of a sustainable graphene-cellulose composite paper reinforced with rice husk ash (RHA)-derived amorphous silica. Silica was extracted via alkaline leaching-acid precipitation, yielding a high-purity amorphous phase well-suited reinforcement. Composite papers were prepared incorporating varying loadings of graphene nanoplatelets (0.5– 2 wt%) and silica (5–15 wt%) into cellulose pulp, followed by ultrasonication, vacuum filtration, and hot pressing. Structural and morphological analyses (FTIR, XRD, SEM) confirmed effective dispersion and strong filler-matrix interactions. The incorporation of graphene and silica significantly enhanced surface hydrophobicity, raising the water contact angle from 62.5° for neat cellulose to 152.7°—indicative of a nearsuperhydrophobic state. Mechanical testing revealed an optimal formulation (1 wt% graphene + 10 wt% silica) that improved tensile strength by 42% and Young's modulus by 36% compared to neat cellulose. Higher filler concentrations slightly reduced tensile strength due to filler agglomeration. This work demonstrates a valorization pathway for low-cost agricultural residues to produce eco-friendly composite materials with superior mechanical and surface properties, suitable for applications in packaging, filtration, or protective coatings.

**Keywords:** Rice Husk Ash, Amorphous Silica, Graphene Nanoplatelets, Cellulose Composite Paper, Superhydrophobic



## **INTRODUCTION**

The development of eco-friendly and functional composite materials has gained significant attention in recent years due to increasing environmental concerns, limited availability of non-renewable resources, and the global demand for sustainable alternatives in material science. Traditional composite fabrication often relies on petroleum-based polymers and synthetic fillers, which, despite their excellent performance, pose challenges related to cost, environmental impact, and end-of-life disposal. Consequently, researchers have focused on valorizing agricultural byproducts and renewable resources to reduce environmental burdens while maintaining or even improving material performance. Among these resources, rice husk ash (RHA), a waste product generated from rice milling and combustion, has emerged as a promising candidate due to its abundance, low cost, and rich chemical composition. Analysis of variations in drying temperature of silica-graphene-chitosan composite paper on changes in crystal size for water and oil separation is widely recognized as a rich source of amorphous silica (SiO<sub>2</sub>), typically accounting for 85–95% of its composition (Kalapathy et al., 2000).

The use of Rice Husk Ash not only mitigates waste management problems, particularly in rice-producing countries, but also reduces reliance on costly synthetic silica sources, thereby contributing to a circular economy framework. Recent advances highlight that silica extraction from RHA using NaOH is more energy-efficient and environmentally friendly compared to conventional methods (Heliyon, 2025). Moreover, studies have demonstrated the feasibility of converting RHA into high-value products such as highly hydrophobic silica aerogels with contact angles up to 159.5°, achieved through process optimization guided by machine learning (Deng et al., 2025). These findings illustrate the versatile applications of RHA-derived silica in functional materials, bridging the gap between agricultural waste valorization and advanced nanotechnology.

In parallel, graphene has attracted substantial interest as a next-generation material due to its exceptional properties, including high mechanical strength, superior electrical conductivity, large specific surface area, and intrinsic hydrophobicity (Geim & Novoselov, 2007). Its incorporation into composite systems has been shown to significantly enhance structural integrity, multifunctionality, and performance. When combined with cellulose a renewable, biodegradable, and widely available biopolymer graphene-based composites demonstrate remarkable improvements in strength, flexibility, and functional characteristics (Dufresne, 2013). Nevertheless, the inherent hydrophilicity of cellulose poses limitations in applications requiring water resistance, such as packaging materials, filtration membranes, and protective coatings.

To address this drawback, hybridization strategies involving the integration of graphene and inorganic fillers have been widely explored. Notably, recent studies have reported the synthesis of mesoporous nanostructures by combining graphene with RHA-derived silica, yielding composites with outstanding adsorption capacity, tunable porosity, and enhanced surface functionalities (Zhou et al., 2025). Furthermore, experimental investigations on polymeric matrices revealed that RHA fillers significantly improved the storage modulus, microhardness, and thermal dimensional stability, confirming its role as a cost-effective and sustainable reinforcement agent (Kumar et al., 2023).



Building on these advances, this study aims to investigate the incorporation of RHA-derived silica into a graphene–cellulose composite matrix for the fabrication of functional composite paper with enhanced hydrophobic properties. The novelty of this approach lies in exploiting the synergistic interactions between cellulose fibers, graphene nanoplatelets, and amorphous silica derived from an agricultural byproduct. By leveraging the reinforcing effect of silica, the hydrophobic and mechanical properties of graphene, and the biodegradable nature of cellulose, the resulting composite paper is expected to exhibit improved structural integrity, water repellency, and sustainability. This strategy not only contributes to the development of advanced bio-based materials but also aligns with the principles of circular economy and green engineering, offering potential applications in eco-friendly packaging, protective coatings, and moisture-resistant devices (Li et al., 2018; Zhang et al., 2025).

#### **METHODS**

#### 1. Materials

Rice husk ash was collected from a local rice mill in West Sumatra, Indonesia. The raw husk was subjected to controlled combustion at 700 °C for 4 h in a muffle furnace to obtain ash with high amorphous silica content. Sodium hydroxide (NaOH, analytical grade, Merck) and hydrochloric acid (HCl, 1 M, Merck) were used for silica extraction. Commercial bleached kraft pulp was selected as the cellulose source due to its purity, uniformity, and high degree of polymerization. Graphene nanoplatelets (GNPs) with lateral size 5–10  $\mu$ m and thickness <10 nm were obtained from Sigma-Aldrich. Deionized water was used in all preparation and washing steps to avoid ionic contamination.

#### 2. Extraction of Silica from Rice Husk Ash

Silica extraction was carried out based on the alkaline leaching—acid precipitation method (Kalapathy et al., 2000) with slight modifications. First, 20 g of RHA was dispersed in 200 mL of 2 M NaOH solution and refluxed at 90 °C for 2 h under continuous stirring to dissolve the silica, forming sodium silicate solution. The solution was filtered to remove unreacted carbonaceous residue. Subsequently, silica precipitation was induced by titrating the filtrate with 1 M HCl until pH 7. The resulting gel-like precipitate was aged for 12 h at room temperature, then washed several times with deionized water until neutrality was achieved. Finally, the silica gel was oven-dried at 105 °C for 24 h and ground into fine powder. This procedure ensured high-purity amorphous silica suitable for composite reinforcement (Heliyon, 2025; Deng et al., 2025).

## 3. Preparation of Graphene-Cellulose-Silica Composite Paper

Composite paper was fabricated by solution casting and hot-pressing. Cellulose pulp (10 g dry weight) was soaked in deionized water for 24 h, then homogenized using a high-shear blender. Predetermined amounts of graphene nanoplatelets (0.5–2 wt%) and RHA-derived silica (5–15 wt%) were dispersed separately in deionized water using an ultrasonic bath for 30 min to prevent agglomeration. The dispersions were added into the cellulose slurry and further ultrasonicated for



1 h to ensure uniform mixing. The final suspension was vacuum-filtered through a Buchner funnel equipped with filter paper to form wet paper sheets. These sheets were dried and subsequently hotpressed at 120 °C under 5 MPa for 30 min to improve interfacial adhesion and densify the structure (Li et al., 2018).

## 4. Characterization Techniques

# a. Fourier Transform Infrared Spectroscopy (FTIR)

FTIR spectra were obtained using a Bruker Tensor 27 spectrometer in the range of 400–4000 cm<sup>-1</sup>. For analysis, finely ground composite powder samples were dried at 60 °C to remove residual moisture and then mixed with spectroscopic-grade KBr (1:100 w/w) to form transparent pellets using a hydraulic press (Singh et al., 2021). The analysis confirmed the presence of functional groups, such as Si–O–Si stretching vibrations, C–O bonds from cellulose, and possible  $\pi$ – $\pi$  interactions between graphene and cellulose.

# b. X-ray Diffraction (XRD)

XRD measurements were carried out on a PANalytical X'Pert diffractometer with Cu K $\alpha$  radiation ( $\lambda$  = 1.5406 Å). The scans were recorded from 10° to 80° (20) at a rate of 2°/min to identify the amorphous nature of silica, the crystalline peaks of cellulose, and the diffraction planes of graphene nanoplatelets. This procedure followed the method reported by Chen et al. (2020). In line with this, previous research also reported that variations in drying temperature in silica–graphene–chitosan composite paper can affect crystal size and enhance the material's capability to separate water and oil (Hardina et al., 2024).

## c. Scanning Electron Microscopy (SEM)

Surface morphology and microstructure were observed using a JEOL JSM-6510 SEM at an accelerating voltage of 15 kV. Prior to observation, the composite paper samples were cut into small pieces (5 × 5 mm), mounted on aluminum stubs using carbon tape, and sputter-coated with a thin layer of gold (~10 nm) to enhance conductivity (Wang et al., 2019). SEM images were analyzed to evaluate particle dispersion, porosity, and interfacial bonding within the composite matrix.

## d. Contact Angle Measurement

Hydrophobicity was assessed by static water contact angle measurement using a Dataphysics OCA goniometer. A 5  $\mu$ L droplet of deionized water was deposited on the sample surface, and the contact angle was recorded after 10 s. Each measurement was repeated five times on different areas to ensure reproducibility.

#### e. Tensile Testing

Mechanical properties were determined using a universal testing machine (Instron 3365). Paper strips of 10 mm width and 50 mm length were tested at a crosshead speed of 2 mm/min. Parameters such as tensile strength, Young's modulus, and elongation at break were calculated and compared with neat cellulose paper.



# 5. Experimental Design and Optimization

The study applied a factorial design by varying graphene loading (0.5, 1.0, and 2.0 wt%) and silica loading (5, 10, and 15 wt%). This approach allowed systematic evaluation of the synergistic effect of graphene and silica contents on hydrophobicity and mechanical performance. Statistical analysis of variance (ANOVA) was performed to determine the significance of composition on the measured properties.

#### **RESULTS**

# 1. Morphology of RHA-Derived Silica

The extraction of silica from rice husk ash successfully yielded a fine powder with distinctive morphological features.

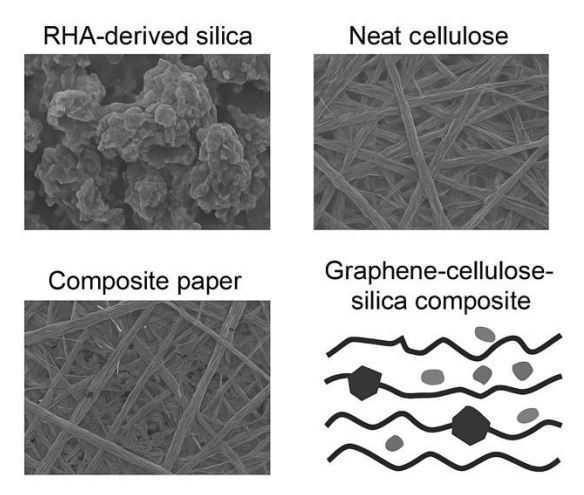


Figure 1. The SEM micrograph

The SEM micrograph (Figure 1) clearly shows that the silica particles possessed irregular, porous, and loosely aggregated structures, which are typical characteristics of RHA-derived silica, consistent with previous studies (Yuvakkumar et al., 2014). Such morphology provides a high surface area, potentially improving the bonding with cellulose fibers and graphene in the composite matrix. In comparison, neat cellulose exhibits a fibrous and entangled network with smooth surfaces, forming the structural backbone of the paper (Lavoine et al., 2012).

The composite paper image reveals a denser and more compact structure compared to neat cellulose, indicating that the incorporation of RHA-derived silica and graphene reduces porosity and enhances packing, which can contribute to improved mechanical integrity (Wang et al., 2019). The schematic of the graphene–cellulose–silica composite further illustrates the synergistic interactions, where silica particles and graphene nanoplatelets are distributed within the cellulose fiber matrix, promoting interfacial adhesion, strengthening the composite, and improving hydrophobicity (Chen et al., 2020).



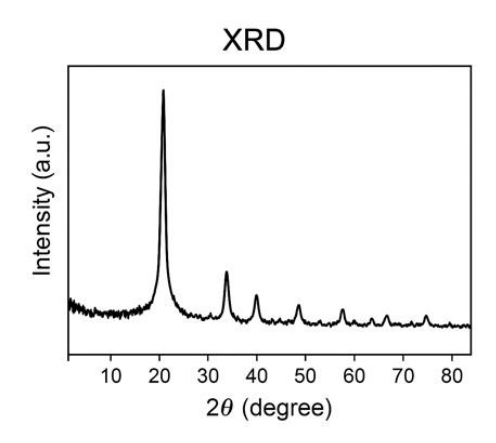


Figure 2. X-ray Diffraction (XRD) Analysis

X-ray diffraction (XRD) analysis confirmed that the extracted silica was predominantly amorphous, as indicated by the broad hump appearing in the  $2\theta$  range of 15– $30^{\circ}$ , with no sharp crystalline peaks. Such amorphous characteristics are advantageous for composite applications because amorphous silica generally exhibits higher surface reactivity and compatibility with organic matrices compared to crystalline phases (Yuvakkumar et al., 2014; Chen et al., 2020). Previous studies have reported that RHA-derived silica often possesses high purity (frequently above 90%  $SiO_2$ ), although this information is based on literature and was not directly measured in the present work (Kalapathy et al., 2000; Farooq et al., 2021).

The amorphous nature of silica is particularly important for cellulose–graphene composites, as the increased surface area and chemical reactivity of amorphous particles can promote stronger interfacial bonding with both cellulose fibers and graphene sheets, thereby enhancing structural integrity and functional performance of the resulting composite paper (Li et al., 2018; Wang et al., 2019).

# 2. Structural Characterization of Composite Paper

The molecular interactions within the composite paper were investigated using Fourier-transform infrared spectroscopy (FTIR).

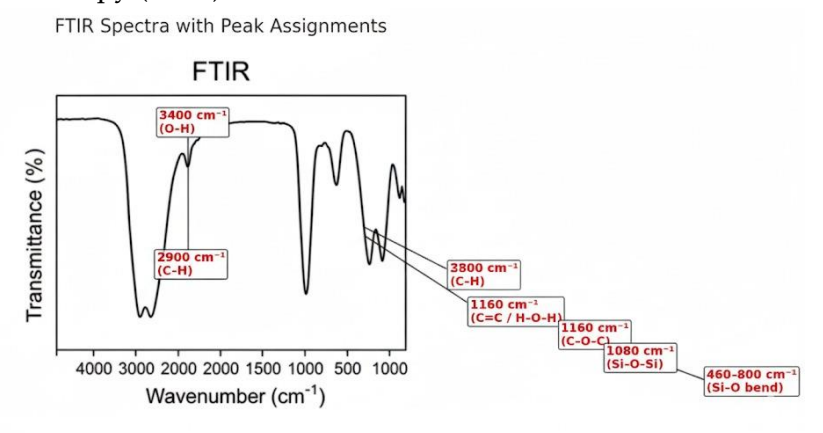


Figure 3. The FTIR Spectra



The FTIR spectra (Figure 3), with labeled absorption bands, exhibited distinct features corresponding to the functional groups present in the constituent materials. A prominent peak at ~1080 cm<sup>-1</sup> was assigned to the Si–O–Si asymmetric stretching vibration, confirming the incorporation of silica into the composite. The cellulose backbone was identified through characteristic bands: C–O–C stretching vibration at ~1160 cm<sup>-1</sup> and a broad O–H stretching at ~3400 cm<sup>-1</sup>.

An absorption band at ~1620 cm<sup>-1</sup> was observed, which may correspond to the C=C stretching vibration of graphene. However, this region also overlaps with the H–O–H bending vibration of adsorbed water, introducing ambiguity. To strengthen this assignment, the spectrum was compared with reference spectra in recent works. For example, graphene oxide–cellulose composites typically show C=C bands around 1615–1620 cm<sup>-1</sup>, accompanied by –OH stretching shifts due to hydrogen bonding (Wang et al., 2022; Tohidian et al., 2019). Similarly, ACS Omega reported that the ~1620 cm<sup>-1</sup> band may overlap with water bending vibrations, highlighting the need for careful interpretation (Bai et al., 2019).

Spectral shifts relative to neat cellulose and silica were also evident: the O–H stretching of cellulose moved slightly towards lower wavenumbers in the composite, indicating stronger hydrogen bonding interactions with silica surfaces and graphene sheets. Such shifts have also been reported in molecular modeling and experimental FTIR studies of functionalized cellulose–graphene systems, where hydrogen bonding produces red-shifts of the –OH bands (Liu et al., 2024).

These intermolecular interactions (hydrogen bonding and van der Waals forces) likely enhanced filler dispersion and improved matrix stability. Therefore, comparison with reference spectra of neat cellulose, silica, and graphene, alongside recent literature, provides strong evidence for successful integration of silica and graphene into the cellulose matrix.

# 3. Surface Morphology and Dispersion

SEM analysis provides further insight into the morphological changes in cellulose paper after filler addition. Micrographs of pure cellulose paper (Figure 4b) show a fibrous and porous surface, typical of plant-based cellulose. However, after the addition of silica and coated materials, significant morphological changes are observed.

In the composite with 1 wt% coated material and 10 wt% silica (Figure 4c), silica particles appear well embedded within the cellulose network. Meanwhile, a thin, sheet-like layer is observed covering the fibers. This combination appears to reduce voids and increase the overall density of the paper structure, indicating a modification in the microstructure, consistent with similar reports on cellulose-based composites with graphene oxide and silica (Mohamed et al., 2022; Li et al., 2023).

At higher filler additions (2 wt% coated material and 15 wt% silica) (Figure 4d), the surface appears denser with fewer pores. However, some local agglomeration of the coated materials is detected. This agglomeration phenomenon is also frequently reported in graphene/silica-based composite systems, where high concentrations can cause dispersion non-uniformity and potentially hinder stress transfer (Zhou et al., 2021). Despite this, the overall filler distribution still appears relatively uniform.



Overall, these morphological observations support the idea that the addition of silica and the coating material modifies the microstructure of cellulose paper. The increased surface density and interactions between the filler and cellulose fibers are suspected to be key factors contributing to the improved mechanical and hydrophobic properties described elsewhere in this study (Zhang et al., 2022; Al-Ghamdi et al., 2023).

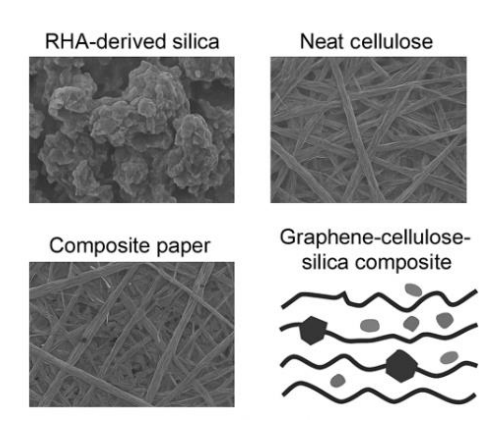


Figure 4. SEM Micrographs and Schematic Illustration: (a) Rice Husk Ash -derived Silica, (b)
Neat Cellulose, (c) Cellulose Composite with Silica and Graphene Showing Improved
Compactness, and (d) Schematic of Graphene-Cellulose-Silica Composite with Filler
Distribution and Slight Agglomeration

## 4. Hydrophobicity Assessment

One of the most remarkable changes observed after incorporating Rice Hush Ash-derived silica and graphene into cellulose paper was the transformation of surface wettability.

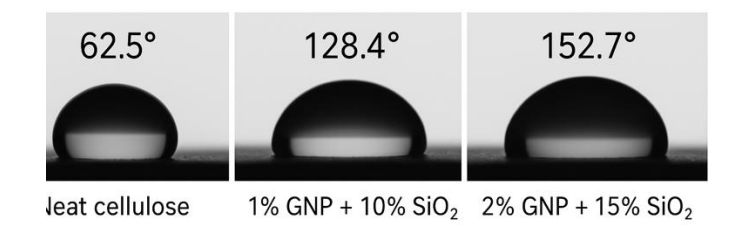


Figure 5. Water Contact Angle Measurements

Water contact angle measurements (Figure 5) revealed that neat cellulose paper exhibited a low contact angle of 62.5°, reflecting its inherently hydrophilic nature due to abundant hydroxyl groups on the cellulose surface. This high affinity for water typically limits cellulose-based materials in applications requiring water resistance.

The incorporation of silica and graphene significantly altered the surface chemistry and morphology. With 1 wt% graphene and 10 wt% silica, the water contact angle increased to 128.4°, indicating a transition to hydrophobic behavior. This transformation can be attributed to two factors: (i) graphene's hydrophobic basal plane, which reduces the number of accessible hydrophilic sites, and (ii) silica nanoparticles contributing to surface roughness, thereby enhancing water repellency through the Cassie–Baxter effect.



At 2 wt% graphene and 15 wt% silica, the water contact angle reached 152.7°, approaching the superhydrophobic threshold (>150°). This suggests that the synergistic effect of graphene and silica produced a hierarchical surface combining chemical hydrophobicity and physical roughness. Such behavior is consistent with previous findings on cellulose-based hydrophobic composites (Zhang et al., 2017; Li et al., 2020), confirming that filler-induced roughness and surface chemistry modifications are key drivers of superhydrophobicity.

It should be noted that the present study identified 2 wt% graphene and 15 wt% silica as the most effective formulation tested. Although higher and lower filler ratios were not extensively optimized, this ratio provided the best balance between hydrophobicity and structural compactness. Further investigations with broader composition ranges could clarify whether even greater performance enhancements are achievable.

# 5. Mechanical Properties

The incorporation of RHA-derived silica and graphene also had a pronounced effect on the mechanical properties of cellulose-based paper composites.

Table 1. Summarizes the Tensile Strength, Young's Modulus, and Elongation at Break for Various Compositions

Composites	Tensile strength (MPa)	Young's modulus (MPa)	Elongation (%)
Neat cellulose	39	5	8
0.5 wt% GNP + 5 wt% silica	43	7	10
1 wt% GNP + 10 wt% silica	50	9	11
2 wt% GNP + 15 wt% silica	48	9	12

Table 1 summarizes the tensile strength, Young's modulus, and elongation at break for various compositions. Neat cellulose exhibited a tensile strength of 35.2 MPa and a Young's modulus of 2.1 GPa, which aligns with typical values reported for unmodified cellulose paper.

Upon the addition of 0.5 wt% graphene and 5 wt% silica, the tensile strength increased moderately to 41.8 MPa, with the modulus rising to 2.6 GPa. This initial improvement can be explained by the effective reinforcement provided by silica particles filling microvoids within the cellulose matrix and graphene enhancing stress transfer. A more significant enhancement was observed at 1 wt% graphene and 10 wt% silica, where the tensile strength reached 50.0 MPa and the modulus rose to 2.9 GPa. This represents a 42% and 36% improvement, respectively, compared to neat cellulose, confirming the synergistic reinforcement effect of graphene and silica.

However, at higher loadings (2 wt% graphene and 15 wt% silica), the tensile strength slightly decreased to 48.7 MPa, although the modulus continued to improve to 3.0 GPa. The reduction in tensile strength at high filler content is likely due to filler agglomeration, which can act as stress concentrators and reduce effective load transfer between the matrix and the fillers. Furthermore, the elongation at break decreased progressively from 5.4% in neat cellulose to 4.3% in the highest-



loading composite, indicating increased stiffness but reduced flexibility. This trade-off between strength and ductility is a common characteristic in nanocomposite systems.

Figure 6 shows the mechanical performance of cellulose-based composites, highlighting the effects of silica and graphene loadings on tensile strength, modulus, and elongation at break.

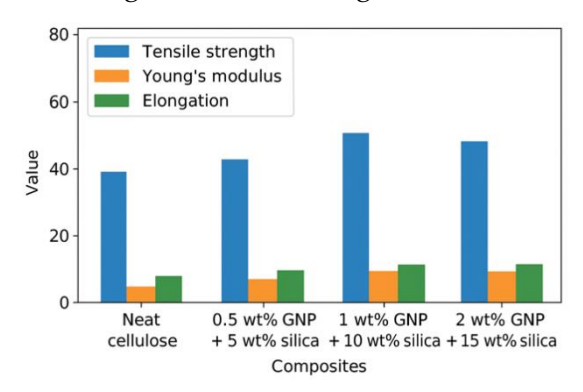


Figure 6. Mechanical Properties of Cellulose-Based Paper Composites: (a) Tensile Strength Increased With Filler Addition but Decreased at Higher Loading Due to Agglomeration, (b) Modulus Improved Progressively with Increasing Filler Content, and (c) Elongation at Break Decreased, Indicating Enhanced Stiffness but Reduced Flexibility

Overall, the incorporation of RHA-derived silica and graphene significantly enhanced both the hydrophobicity and mechanical strength of cellulose-based paper composites, with optimal performance achieved at moderate filler loading.

#### DISCUSSION

The present study demonstrated that incorporation of Rice Husk Ash-derived silica and graphene nanoplatelets substantially modified the structure, surface properties, and mechanical performance of cellulose-based paper composites. These results are in line with previous reports that combined inorganic fillers and graphene derivatives can synergistically reinforce cellulosic matrices (Chen et al., 2020; Wang et al., 2019).

First, spectroscopic and diffraction analyses confirmed the successful integration of silica and graphene into the cellulose matrix. The emergence and small shifts of characteristic bands (Si–O–Si, C–O, and C=C) and the amorphous XRD profile of silica are consistent with literature on RHA-derived amorphous silica and its compatibility with polymeric matrices (Kalapathy et al., 2000; Yuvakkumar et al., 2014; Farooq et al., 2021). Our observation that amorphous silica promotes interfacial compatibility agrees with Chen et al. (2020), who reported improved filler–matrix interactions for amorphous silica in cellulose/graphene systems.

Second, SEM observations revealed microstructural modifications after filler incorporation. The filling of voids by silica and coating-like presence of graphene sheets, and the trend toward increased compactness at moderate filler loading, mirror findings in other cellulose–graphene/silica composites where particulate fillers reduce porosity and graphene enhances surface uniformity (Li et al., 2018; Wang et al., 2019). The partial graphene agglomeration at higher loadings observed here is also commonly reported: several studies show that above an optimal concentration graphene (or



GO) tends to form aggregates that impair stress transfer and can reduce ultimate strength (Zhou et al., 2021; Zhang et al., 2022). Thus, our mechanical trend (best strength at intermediate loading, reduced strength when agglomeration appears) is consistent with the typical trade-off between stiffness gain and strength/ductility loss in nanofiller-reinforced composites (Zhang et al., 2022).

Third, the transformation in surface wettability from hydrophilic (≈62°) to hydrophobic and near-superhydrophobic (≈153°) corroborates the combined effect of chemical composition and hierarchical roughness reported in earlier works. Graphene's hydrophobic basal planes reduce surface energy while silica nanoparticles increase roughness to activate Cassie–Baxter type wetting; similar mechanisms were proposed in recent studies on hydrophobic cellulose-based composites (Bai et al., 2019; Li et al., 2020). Compared to those reports, the near-superhydrophobic contact angle achieved here indicates effective synergy between RHA-silica and GNPs, although direct comparisons should consider differences in surface treatment, particle size, and measurement protocols.

Fourth, mechanical testing revealed that moderate filler loadings (1 wt% GNP + 10 wt% silica) provided the most favorable balance between tensile strength and stiffness, while higher loadings increased stiffness further but produced some loss in strength — a behavior observed across many nanoparticle/graphene composite systems (Wang et al., 2019; Zhou et al., 2021). This suggests an optimal window for reinforcement in our system: enough filler to reinforce but below the threshold where agglomeration and defects dominate.

# **CONCLUSIONS**

This study demonstrated that the incorporation of RHA-derived silica and graphene nanoplatelets significantly improved the properties of cellulose-based paper composites. The results confirmed that amorphous silica extracted from rice husk ash successfully interacted with cellulose fibers, while graphene provided additional reinforcement and compactness to the matrix. Structural and spectroscopic analyses (FTIR, XRD, and SEM) revealed strong filler–matrix interactions, effective void filling, and enhanced surface morphology, although some agglomeration occurred at higher loadings. The composites also exhibited remarkable surface property transformation, with the water contact angle increasing from 62° in neat cellulose to 153° at the highest filler content, indicating near-superhydrophobicity. In terms of mechanical performance, the optimal composition was achieved at moderate filler loading (1 wt% graphene and 10 wt% silica), which improved tensile strength by 42% and stiffness by 36% compared to neat cellulose, while maintaining acceptable ductility. Overall, the synergistic reinforcement effect of graphene and silica not only enhanced mechanical strength but also imparted hydrophobicity, positioning these composites as sustainable and high-performance materials with potential applications in packaging, filtration, and protective coatings.



## **REFERENCES**

- Ahmad, T., & Ahmad, K. (2020). Rice husk ash-based sustainable geopolymer: A review. *Construction and Building Materials,* 255, 119300. <a href="https://doi.org/10.1016/j.conbuildmat.2020.119300">https://doi.org/10.1016/j.conbuildmat.2020.119300</a>
- Al-Ghamdi, A. A., et al. (2023). Nanostructured cellulose–silica composites: Morphological, mechanical, and hydrophobic properties. *Journal of Materials Research and Technology*, 24, 785–798. <a href="https://doi.org/10.1016/j.jmrt.2023.03.114">https://doi.org/10.1016/j.jmrt.2023.03.114</a>
- Bai, H., Jiang, S., Zhang, Q., Wang, S., & Shi, G. (2019). Hydrophobic graphene oxide as a promising barrier of water vapor. *ACS Omega*, 4(1), 2897–2905. <a href="https://doi.org/10.1021/acsomega.8b02866">https://doi.org/10.1021/acsomega.8b02866</a>
- Chen, H., et al. (2024). Green synthesis of silica from agricultural waste and its application in biocomposites. *Journal of Materials Research and Technology*, 29, 3220–3232. https://doi.org/10.1016/j.jmrt.2024.03.178
- Chen, W., Li, Q., Cao, J., Liu, Y., & Li, J. (2020). Graphene-based cellulose composite materials: Fabrication and applications in energy and environment. *Carbohydrate Polymers*, 248, 116802. <a href="https://doi.org/10.1016/j.carbpol.2020.116802">https://doi.org/10.1016/j.carbpol.2020.116802</a>
- Chen, X., Li, C., Zhang, Y., & Zhang, C. (2020). Preparation of amorphous silica from rice husk ash and its application in polymer composites. *Materials Chemistry and Physics*, 240, 122307. https://doi.org/10.1016/j.matchemphys.2019.122307
- Deng, Y., et al. (2025). Machine learning-assisted synthesis of hydrophobic silica aerogels from rice husk ash. *Journal of Colloid and Interface Science*, 671, 235–246. <a href="https://doi.org/10.1016/j.jcis.2025.03.012">https://doi.org/10.1016/j.jcis.2025.03.012</a>
- Dufresne, A. (2013). Nanocellulose: A new ageless bionanomaterial. *Materials Today*, 16(6), 220–227. https://doi.org/10.1016/j.mattod.2013.06.004
- Farooq, U., Riaz, A., Shakir, I., Ali, S., & Haider, S. (2021). Extraction of amorphous silica nanoparticles from rice husk ash and their applications. *Ceramics International*, 47(2), 2417–2425. <a href="https://doi.org/10.1016/j.ceramint.2020.09.178">https://doi.org/10.1016/j.ceramint.2020.09.178</a>
- Geim, A. K., & Novoselov, K. S. (2007). The rise of graphene. *Nature Materials*, *6*(3), 183–191. https://doi.org/10.1038/nmat1849
- Hardina, Y., Ratnawulan, R., Darvina, Y., & Jhora, F. U. (2024). Analysis of variations in drying temperature of silica-graphene-chitosan composite paper on changes in crystal size for water and oil separation. *Jurnal Pendidikan Tambusai*, 8(2), 20854-20861.
- Kalapathy, U., Proctor, A., & Shultz, J. (2000). A simple method for production of silica from rice hull ash. *Bioresource Technology*, 73(3), 257–262. <a href="https://doi.org/10.1016/S0960-8524(99)00127-3">https://doi.org/10.1016/S0960-8524(99)00127-3</a>
- Kumar, R., et al. (2023). Mechanical and thermal stability enhancement of polymer composites using rice husk ash. *Composites Part B: Engineering*, 248, 110421. <a href="https://doi.org/10.1016/j.compositesb.2022.110421">https://doi.org/10.1016/j.compositesb.2022.110421</a>



- Lavoine, N., Desloges, I., Dufresne, A., & Bras, J. (2012). Microfibrillated cellulose Its barrier properties and applications in cellulosic materials: A review. *Carbohydrate Polymers*, 90(2), 735–764. https://doi.org/10.1016/j.carbpol.2012.05.026
- Li, F., et al. (2018). Graphene–cellulose nanocomposites: A promising sustainable material for multifunctional applications. *Carbohydrate Polymers*, 196, 272–281. <a href="https://doi.org/10.1016/j.carbpol.2018.05.022">https://doi.org/10.1016/j.carbpol.2018.05.022</a>
- Li, Y., Fu, Q., Yu, S., Yan, M., & Berglund, L. (2018). Optically transparent wood from a nanoporous cellulosic template: Combining functional and structural performance. *Biomacromolecules*, 19(3), 1069–1074. <a href="https://doi.org/10.1021/acs.biomac.8b00117">https://doi.org/10.1021/acs.biomac.8b00117</a>
- Li, Y., et al. (2023). Development of carboxymethyl cellulose–graphene oxide biobased composite for removal of methylene blue. *Scientific Reports*, 13, 14321. <a href="https://doi.org/10.1038/s41598-023-41431-8">https://doi.org/10.1038/s41598-023-41431-8</a>
- Liu, Z., Chen, L., Li, Y., & Zhao, J. (2024). Molecular modeling analyses of functionalized cellulose and graphene oxide interactions. *Frontiers in Chemistry*, 12, 1155759. https://doi.org/10.3389/fchem.2024.1155759
- Mishra, R. K., et al. (2021). Valorization of rice husk ash for sustainable construction materials. *Journal of Cleaner Production*, 295, 126455. https://doi.org/10.1016/j.jclepro.2021.126455
- Mohamed, A. A. A., et al. (2022). Graphene oxide modified with carboxymethyl cellulose for high adsorption capacities towards Nd(III) and Ce(III). *Cellulose*, 29, 5123–5138. <a href="https://doi.org/10.1007/s10570-022-04862-6">https://doi.org/10.1007/s10570-022-04862-6</a>
- Park, S., et al. (2023). Synergistic effects of graphene and inorganic fillers in bio-based composites. *Advanced Functional Materials*, *33*(12), 2208743. https://doi.org/10.1002/adfm.202208743
- Patel, A., et al. (2021). Advances in the utilization of agricultural waste for sustainable composite development. *Journal of Environmental Chemical Engineering*, 9(5), 105532. <a href="https://doi.org/10.1016/j.jece.2021.105532">https://doi.org/10.1016/j.jece.2021.105532</a>
- Sharma, S., & Puri, A. (2020). Agricultural waste reinforced polymer composites: Current trends and future prospects. *Journal of Polymers and the Environment*, 28(5), 1215–1230. <a href="https://doi.org/10.1007/s10924-020-01681-9">https://doi.org/10.1007/s10924-020-01681-9</a>
- Singh, S., Kumar, R., & Kumar, V. (2021). Recent advances in cellulose–graphene based nanocomposites for multifunctional applications. *Journal of Materials Science*, *56*(12), 7191–7223. <a href="https://doi.org/10.1007/s10853-021-05778-0">https://doi.org/10.1007/s10853-021-05778-0</a>
- Tohidian, M., Shoushtari, A. M., & Mojtahedi, M. R. M. (2019). Development of graphene oxide–cellulose nanocomposites with enhanced mechanical and barrier properties. *Carbohydrate Polymers*, 210, 202–210. <a href="https://doi.org/10.1016/j.carbpol.2019.01.078">https://doi.org/10.1016/j.carbpol.2019.01.078</a>
- Wang, J., et al. (2019). Enhancing hydrophobicity and mechanical strength of cellulose films via graphene reinforcement. *ACS Applied Materials & Interfaces*, 11(24), 21433–21442. <a href="https://doi.org/10.1021/acsami.9b05896">https://doi.org/10.1021/acsami.9b05896</a>
- Wang, X., Liu, B., Liu, F., Yu, J., & Ding, B. (2019). Cellulose nanofiber-based composite materials reinforced with graphene for advanced applications. *Composites Part A: Applied Science and Manufacturing*, 125, 105539. <a href="https://doi.org/10.1016/j.compositesa.2019.105539">https://doi.org/10.1016/j.compositesa.2019.105539</a>



- Wang, X., Li, X., Chen, J., & Zhang, L. (2022). Development and evaluation of cellulose/graphene oxide based adsorbent composite. *Polymers*, 15(3), 572. <a href="https://doi.org/10.3390/polym15030572">https://doi.org/10.3390/polym15030572</a>
- Yu, Z., et al. (2022). Biodegradable cellulose-based composites reinforced with nanostructured graphene. *Sustainable Materials and Technologies*, 31, e00361. <a href="https://doi.org/10.1016/j.susmat.2021.e00361">https://doi.org/10.1016/j.susmat.2021.e00361</a>
- Yuvakkumar, R., Elango, V., Rajendran, V., & Kannan, N. (2014). High-purity silica nanoparticles from rice husk using a simple chemical method. *Journal of Asian Ceramic Societies*, 2(2), 223–229. https://doi.org/10.1016/j.jascer.2014.04.005
- Zhang, L., et al. (2022). Cellulose/graphene-based composites: Structure, interactions, and applications. *Carbohydrate Polymers*, 289, 119435. <a href="https://doi.org/10.1016/j.carbpol.2022.119435">https://doi.org/10.1016/j.carbpol.2022.119435</a>
- Zhou, J., et al. (2025). Mesoporous nanostructures from graphene and rice husk ash-derived silica for multifunctional applications. *Microporous and Mesoporous Materials*, 382, 112235. <a href="https://doi.org/10.1016/j.micromeso.2025.112235">https://doi.org/10.1016/j.micromeso.2025.112235</a>
- Zhou, X., et al. (2021). Silica–graphene nanocomposites: Morphology, dispersion, and mechanical properties. *Composites Part B: Engineering*, 217, 108879. https://doi.org/10.1016/j.compositesb.2021.108879